Some Accuracy Limiting Effects in an Atomic Beam Frequency Standard

Robert J. Harrach

National Bureau of Standards, Boulder, Colorado

Abstract

The accurate resonance frequency of the transition $(F, M_F) = (4, 0) \leftrightarrow (3, 0)$ in the ground state of cesium-133 is expressed in the form of an operational equation for an atomic beam spectrometer. Emphasized are the terms in this equation which correct for the beam direction dependence and radiation field dependence of measured resonance frequencies:

$$\tfrac{1}{2}\{\nu_{res_i}(P_1) + \nu_{res_j}(P_1)\} - \tfrac{1}{2}(S_i + S_j)\, P_1 ,$$

where i and j refer to opposite beam directions through the apparatus, P_1 is the microwave power exciting the transition, and S_i and S_j are the rates of linear frequency shift. The results of a detailed theoretical analysis are given which specify the contributions to these terms by various apparatus and fundamental shift-inducing effects.

This approach to accuracy specification is applied to the United States frequency standard, a National Bureau of Standards atomic beam machine designated NBS III, through a set of experiments using an atomic hydrogen maser as a highly stable reference frequency source. The corrections determined are -3.2×10^{-12} for beam direction dependence, -2.2×10^{-12} for power dependence, and $+ 0.4 \times 10^{-12}$ for second-order Doppler shift. The uncertainties in these corrections and contributions from other sources give a present 1σ estimate of accuracy capability of $\pm 1.1 \times 10^{-12}$ for NBS III. This figure should be reducible by one order of magnitude through efforts to eliminate systematic errors in the measurements of ν_{res_i} and ν_{res_j}.

Up to the present time the lowest inaccuracy figure that has been quoted[1] for any frequency standard is $\pm 1.1 \times 10^{-12}$ as a single standard deviation (1σ) estimate for a National Bureau of Standards cesium beam machine designated NBS III. Attempts to improve on this value are resisted by the difficulty in identifying and making corrections for resonance frequency shifts induced by a variety of effects.

Intrinsic or fundamantal effects originate from the motion of atoms (Doppler effect), the structure of atoms (effect of neighboring energy levels), and properties of the transition-inducing radiation field (Bloch-Siegert and Stark effects). But the frequency shifts these generate are relatively feeble. Other effects are present because the atomic beam apparatus falls short of ideality. As examples, the phases of the pair of separated radiation fields are not exactly equal, the radiation fields are not strictly monochromatic, and the static magnetic c-field is not precisely uniform. The frequency shifts due to such "apparatus effects" establish the present limits of accuracy.

In this paper we consider a set of high precision experiments which enable identification of the particular effects which are most significant in limiting the accuracy of the NBS III beam machine. This work is one segment of a detailed study of atomic beam resonance frequency shifts.[2]

The standard of frequency is defined by the transition $(F, M_F) = (4, 0) \leftrightarrow (3, 0)$ in the ground state of cesium-133, for which the unshifted resonance frequency (Bohr frequency) is

$$\nu_B(H_c) \simeq \nu_B(0) + (426.4) H_c^2 , \qquad (1)$$

where H_c is the magnitude of a weak external magnetic field (in oersteds), and $\nu_B(0) \equiv 9,192,631,770$ cps. In Table 1 a summary is given of some of the resonance frequency shifts which are calculated for this transition. The notation $(\alpha, \ell, L, \nu_0, \bar{\nu}_0)$ used in the Table is the same as that used by Ramsey.[3] In particular, $\bar{\nu}_0$ and ν_0 are the Bohr frequencies corresponding to the average square c-field magnitudes in the drift region and transition regions, respectively.

The predicted frequency shifts depend on the level of microwave input power (P) exciting the transition, and on the beam direction through the apparatus (via the phase difference δ). This suggests the utility of relating the accurate frequency, $\nu_B(0)$, and measured resonance frequencies with an operational equation:

$$\nu_B^{(0)} = \tfrac{1}{2}\{\nu_{res_i}(P_1, \bar{H}_{c_1}) + \nu_{res_j}(P_1, \bar{H}_{c_1})\} - (426.4)\bar{H}_{c_1}^2 - (426.4)(\overline{H^2}_{c_1} - \bar{H}_{c_1}^2)$$

$$- \tfrac{1}{2}(S_i + S_j)P_1 - \delta\nu_{Doppler} - \delta\nu_{c\text{-field}} - \cdots\cdots . \qquad (2)$$

The subscripts i and j refer to opposite beam directions through the apparatus, P_1 is the microwave input power which excites the transition, and $\bar{H}_{c_1}$ is the average c-field magnitude. The first term is just the mean frequency for opposite beam directions, and is aimed at eliminating the effect of phase difference. The second term corrects to zero magnetic field, and the third term adjusts for the use of $\bar{H}_c^2$ in the c-field calibration, rather than H_c^2. The fourth term corrects for effects which give a linear power-dependent shift that vanishes in the limit of zero excitation intensity and is independent of beam direction. (This includes four items in Table 1.) S_i and S_j are experimentally determined slopes (in cps per milliwatt, say) of a linear component of the observed frequency shifts. The fifth term subtracts out the second-order Doppler shift (given by Fig. 3), and the sixth term takes account of the distortion of the resonance due to inequality of the c-field magnitudes in the transition and drift regions (Fig. 2). The relation should be continued to include other contributions[6] which are not explicitly treated here, e. g., physical overlap, cavity pulling, multiplier chain transient phase shifts, and various servo system effects.

The set of experiments with the NBS III beam spectrometer were performed using an atomic hydrogen maser from Varian Associates as a highly stable reference frequency source.[1] The dependence of the $(4, 0) \longleftrightarrow (3, 0)$ resonance frequency on radiation field intensity was measured, under varied conditions of beam direction through the apparatus, c-field magnitude, and excitation spectrum.

The power-dependent frequency shifts observed for three successive reversals of the beam direction are shown in Fig. 4. Over the range of excitation intensities considered the shifts are linear, and data for opposite beam directions show a slightly different slope and a relative frequency offset. The important features of the data are the slopes, zero power (extrapolated) intercepts, and the average values of these quantities for

opposite beam directions. These are summarized in Table 2.

The interpretation of these results is found in terms of apparatus, rather than fundamental, effects. Evaluating the very small expected shifts due to the latter, using $\ell = 1.02$cm, $L = 366$ cm, and $\alpha = 2.3 \times 10^4$cm/sec in Table 1, we have:

neighboring levels effect: $\delta\nu/\bar{\nu}_0 \simeq + (7.6) \times 10^{-16} \tan^2(\eta) P/P_0$

Bloch-Siegert effect: $\delta\nu/\bar{\nu}_0 \simeq + (3.8) \times 10^{-16} P/P_0$

Stark effect: $\delta\nu/\bar{\nu}_0 \simeq - (1.5) \times 10^{-18} P/P_0$

2nd-order Doppler effect: $(\delta\nu/\bar{\nu}_0)_{P_0} = - 4.4 \times 10^{-13}$.

The observed shifts are roughly $+ 3 \times 10^{-12} P/P_0$, with $P_0 \simeq 6.0$mW.

The relative displacement of the resonance frequency for opposite beam directions is attributed to a phase difference between the radiation fields. If the beam experiences a phase difference δ_i for one direction and δ_j for the other, the frequency difference is $\Delta\nu = \alpha(\delta_i - \delta_j) / 2\pi L$. For $\delta j = - \delta_i$, the successive beam reversals would give a reproducible frequency difference. This was clearly not the case. For either beam direction the phase difference value was of order 10^{-3} radian, but in reversing the beam direction its precise magnitude was changed. It is felt that this irreproducibility is a consequence of the system being exposed to atmospheric pressure in order to interchange the oven and detector. Contaminants in the cavity ends which can contribute to a phase difference value then interact with air and moisture, resulting in a modified value. This circumstance can be avoided by designing the system so that it may be kept under vacuum while the oven-detector interchange is made. Both an oven and detector could be situated at each end of the apparatus, with adjustments for positioning the components so that either combination of oven and detector could be used.

The average rate of frequency shift for opposite beam directions was reproducible, with the magnitude

$$\frac{1}{2\bar{\nu}_o} (S_i + S_j) \simeq + 5.6 \times 10^{-13}/\text{mW}. \qquad (3)$$

Inbalance between pairs of sidebands in the excitation spectrum provides an interpretation of this result. A spectrum analysis revealed that the brightest sidebands were 44 db below the primary intensity at ± 60 cps and ● 120 cps

away from the primary frequency. Each pair was balanced to within an uncertainty of 2 db. If the sideband at - 60 cps was 1 to 2 db above that at + 60 cps, then the expression in Table 1 predicts a fractional shift of + 2.0 to + 4.5 parts in 10^{13} per milliwatt. Similarly, this inbalance in the ± 120 cps components would give an additional contribution half as large. When the excitation spectrum was changed, by using a different multiplier chain, the rate of shift was altered by more than a factor of two, confirming the interpretation as a spectrum effect.

The small beam direction-dependent contribution to the rate of shift,

$$\frac{1}{2\bar{\nu}_0}(S_i - S_j) \simeq 1.0 \times 10^{-13}/\text{mW}, \qquad (4)$$

is not satisfactorily understood. Phase difference is capable of making such a contribution, but the sign is wrong to account for the observations. A possible explanation is found in terms of a first-order Doppler shift due to leakage radiation from the cavity end slots into the drift region, but this has not been convincingly demonstrated.

Supplementary experiments indicated that the power-dependence of the resonance is unaffected by increasing the c-field magnitude above the 1/20 0e operating level, and by reversing c-field polarity. The displacements in the resonance frequency which accompanied performance of these operations were consistent with expectations based on the quadratic c-field dependence. For example, a residual average field component, $\bar{H}_0(x)$, along the direction of the applied c-field, $\bar{H}_a(x)$, causes the resultant c-field magnitude to change by approximately $2\bar{H}_o(x)$ when the polarity of the applied field is reversed. This shifts the (4, 0) ←→ (3, 0) resonance frequency by about $(426.4)4\bar{H}_a(x)\bar{H}_o(x)$ cps, and the shift is removed when the applied field component is adjusted to restore the net c-field to its original value. From these supplementary experiments, we conclude that physical overlap of neighboring resonances, the Millman effect,[3] and the c-field difference quantity, $\bar{H}_c(\ell) - \bar{H}_c(L)$, make negligible frequency shift contributions.

The foregoing analysis determines the frequency corrections that should be applied to the NBS III standard, and helps to establish the limits of accuracy uncertainty. The device is normally operated with an input

power of 4.0 milliwatts, a c-field magnitude of 0.0484 Oe, and with a beam direction corresponding to experiments (2) and (4) in Table 2. The correction for power-dependence, using equation (3) and $P_1 = 4.0$ mW, is then

$$-\frac{1}{2\bar{\nu}_o}(S_i + S_j)P_1 \simeq -2.2 \times 10^{-12}.$$

A second-order Doppler shift was too small to be resolved in the experiments, but a correction can be made on theoretical grounds. Using Fig. 3 for $P_1 = 2P_o/3$, and $\alpha \simeq 2.3 \times 10^4$ cm/sec, we have

$$-\frac{1}{\bar{\nu}_o}(\delta\nu_{\text{Doppler}})P_1 \simeq +0.4 \times 10^{-12}.$$

Similarly, the shift due to c-field distortion was beyond experimental resolution. Calibrated line shape traces of the field-sensitive transitions, $(4,\pm 1) \leftrightarrow (3,\pm 1)$, showed that $|\bar{H}_c(\ell) - \bar{H}_c(L)| < 2 \times 10^{-3}$ Oe, so a theoretical upper limit for the correction magnitude is calculated, using the expression in Table 1 with $H_{c_1} = 0.0484$ Oe, to be less than 3×10^{-14}.

The most important, but most poorly defined correction is that for beam direction-dependence. A reasonable approach is to make this correction with respect to the average of the three determinations of $\frac{1}{2}(\nu_{\text{res}_i} + \nu_{\text{res}_j})$. Then, for example, if the beam has the orientation of experiment 2 in Table 2, the appropriate correction is -3.2×10^{-12}, with a maximum uncertainty estimated from the data to be no more than $\pm 2.4 \times 10^{-12}$ (three times the rms deviation). However, if the beam machine is left undisturbed in a given orientation for long periods of time, this phase difference correction whould be considered to be much more uncertain.

The assessment of total accuracy uncertainty is made by considering the individual uncertainties in the terms that make up equation (2). An itemized account for the NBS III standard, including a discussion of the way that individual contributions should be combined to arrive at a total estimate, has been given by Beehler, et al.[6] A similar tabulation for NBS III, taking account of the results of this paper, is given in Table 3. The single standard deviation estimate of accuracy capability is approximately $\pm 1.1 \times 10^{-12}$.

The designation "accuracy capability" is meant to imply the limits of uncertainty when a set of evaluative experiments are performed, as distinct from undisturbed, routine operation of the standard.

The increasing availability of frequency devices (atomic beams and masers) capable of stabilities of a few parts in 10^{13} over a long duration (100 hours or more) gives promise of improved accuracies. A systematic experimental investigation using a reference frequency source of this high precision has not been carried out to evaluate most of the uncertainty factors in Table 3. Especially in the cases of miscellaneous servo system effects, multiplier chain phase shifts, and the first-order Doppler effect, it is lack of information which makes the estimated uncertainties as large as they are. These experiments, coupled with efforts to reduce systematic errors in the measurements of ν_{res_i} and ν_{res_j} (for which the installation of the alternate oven-detector system mentioned earlier would be a starting point) can reasonably be expected to improve the NBS III accuracy capability figure by an order of magnitude.

ACKNOWLEDGMENTS

I wish to express my gratitude to R. E. Beehler for many helpful discussions during the course of this work. The experiments which have been described were performed by him, D. J. Glaze, and C. S. Snider.

REFERENCES

(1) R. Beehler, D. Halford, R. Harrach, D. Allan, D. Glaze, C. Snider, J. Barnes, R. Vessot, H. Peters, J. Vanier, L. Cutler, L. Bodily, "An intercomparison of atomic standards, "Proc. IEEE (Letter), 54, 301-302, February 1966.

(2) R. Harrach, "Radiation field dependent frequency shifts of atomic beam resonances," to be published.

(3) N. Ramsey, MOLECULAR BEAMS. London, England: Oxford University Press, 1956.

(4) N. Ramsey, "Shapes of molecular beam resonances," in RECENT RESEARCH IN MOLECULAR BEAMS (I. Estermann, ed.). New York: Academic Press, 1959.

(5) R. Haun, Jr. and J. Zacharias, "Stark effect on Cs-133 hyperfine structure, "Phys. Rev., 107, 107-109, July 1957.

(6) R. Beehler, R. Mockler, and J. Richardson, "Cesium beam atomic time and frequency standards," Metrologia, 1, 114-131, July 1965.

TABLE 1

approximate shift, $(\omega_{res} - \bar{\omega}_o)$, at optimum excitation intensity, in cps.	Effect	Power-dependence	Reference
$-\alpha^2/2L$	Phase difference, $\phi_2 - \phi_1 = \alpha$(rad) where 1 and 2 refer to first and second radiation fields	Fig. 1	(2)
$+ \alpha(\omega_o - \bar{\omega}_o)/L =$ $- \frac{\alpha}{L}(426.4)\bar{H}_c(i)\,\bar{H}_c(i) - \bar{H}_c(L)]$	c-field non-uniformity, which makes the average field magnitude in the drift region, $\bar{H}_c(L)$, differ from the average magnitude in the transition regions, $\bar{H}_c(i)$	Fig. 2	(2)
$+ \frac{\alpha(0.045)\alpha^2 \cdot 4}{i \cdot 4L(\omega_o - \omega_1)}$	Sidebands in an impure excitation spectrum. The ratio of the intensity of the sideband at frequency ω_1 to the primary intensity at $\bar{\omega}_o$ is $\alpha_i = P_{sb}/P$. The optimum primary intensity is P_o(in mw, say).	linear; take times P/P_o	(4),(2)
$- \bar{\omega}_o 3\alpha^2/4c^2$	Second-order Doppler effect; c = speed of light	Fig. 3	(2)
$+ \frac{(0.09)\alpha^2}{4L\bar{\omega}_o}$	Bloch-Siegert effect	linear; take times P/P_o	(3)
$- \frac{\alpha}{L}(2.29)10^{-1}\overline{E_o^2}$	Stark effect; $\overline{E_o^2}$ is the mean square electric field component when the radiation field is at optimum intensity	linear; take times P/P_o	(5)
$+ \frac{(0.045)\alpha^2\tan(\epsilon)}{4L\bar{\omega}_o}$	Neighboring levels; ϵ is the angle between the oscillating radiation field and the static c-field	linear; take times P/P_o	(4),(2)

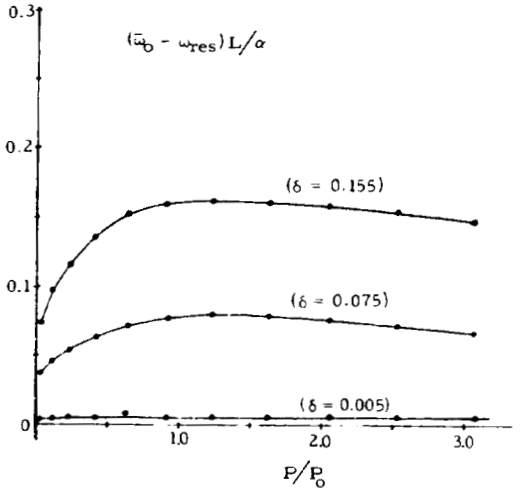

Fig. 1 Theoretical frequency shift induced by a small phase difference, δ(radians), as a function of excitation intensity.

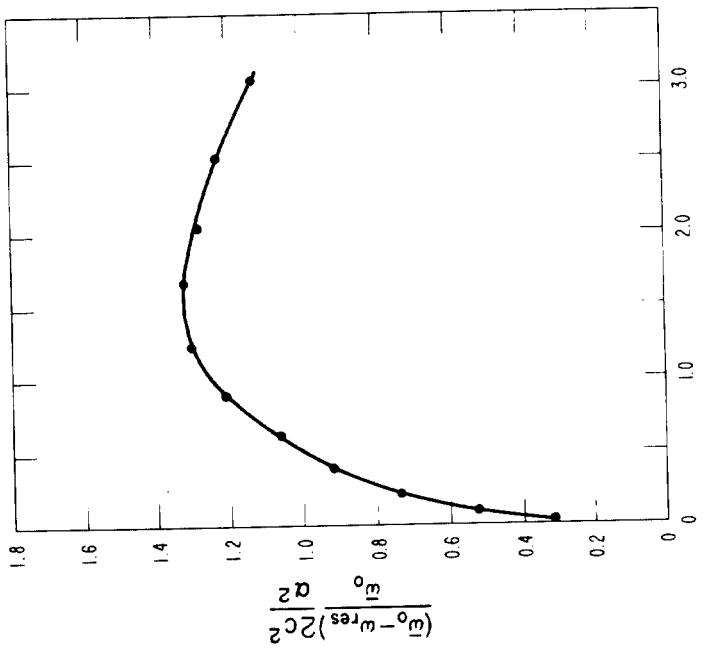

Fig. 3 Theoretical frequency shift due to a second-order Doppler effect, as a function of excitation intensity

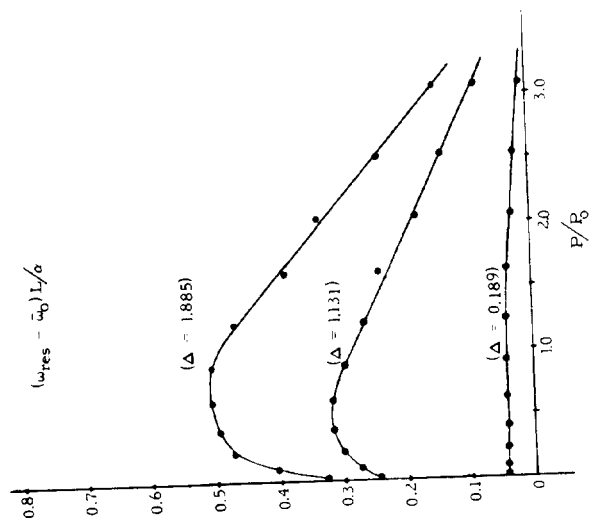

Fig. 2 Theoretical frequency shift induced by c-field non-uniformity which makes $\nu_o \neq \bar{\nu}_o$. The parameter labeling the curves is $\Delta = 8\pi L(\nu_o - \bar{\nu}_o)/\alpha$.

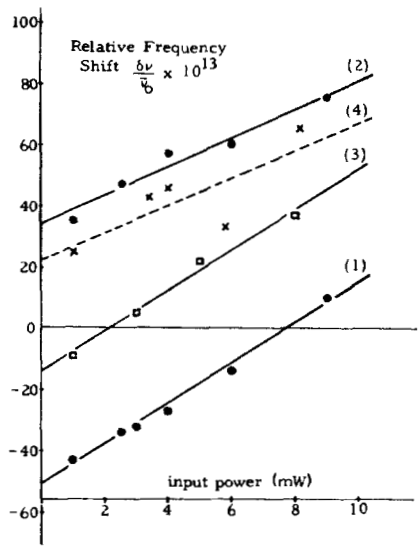

Fig. 4 Power-dependent frequency shifts of the (4,0)↔(3,0) transition in the NBS III atomic beam spectrometer. The least squares determined lines (1) and (3) represent one beam direction, and (2) and (4) the other, in chronological order. The zero point for the frequency shift relative to the H-maser reference is arbitrarily chosen. The data points for lines (1), (2), and (3) are means for 1/2 hour averaging times with standard deviations of 2 to 4 parts in 10^{13}. Line (4) was determined in a more brief experiment. The time duration between successive experiments was about 5 days.

TABLE 2

Summary of experimental results in Fig. 4. The slopes and intercepts, together with their standard deviations, are derived by least squares analysis

Experiment	Slope, S (parts in 10^{13}/mW)	Avg. slope, $\frac{1}{2}(S_1+S_3)$ (parts in 10^{13}/mW)	Difference slope $\frac{1}{2}(S_1-S_3)$ (parts in 10^{13}/mW)	Zero power intercept (parts in 10^{13})	Avg. zero power intercept (parts in 10^{13})
1	6.58 ± 0.32	5.63 ± 0.33	0.96 ± 0.33	- 51.3 ± 1.6	- 8.8 ± 1.7
2	4.67 ± 0.58	5.67 ± 0.40	1.00 ± 0.40	+ 33.8 ± 3.0	+ 9.6 ± 2.0
3	6.66 ± 0.53	5.58 ± 0.78	1.08 ± 0.78	- 14.6 ± 2.7	+ 3.9 ± 4.0
4	4.49 ± 1.49			+ 22.3 ± 7.5	

TABLE 3

Contributions to inaccuracy for NBS III cesium beam frequency standard

Source	3σ estimate in parts in 10^{12}
Uncertainty in $\bar{H}_c$	± 0.3
Use of $\bar{H}_c^2$ for $\overline{H_c^2}$	± 0.1
Uncertainty in *1st- and 2nd-order Doppler shifts*	± 0.3
Distortion from $\bar{H}_c(t) \neq \bar{H}_c(L)$	± 0.1
Uncertainty in c-field polarity dependent shifts	± 0.3
Uncertainty in cavity phase difference	± 2.4
Cavity mistuning	± 0.1
Overlap of neighboring transitions	± 0.3
Uncertainty in power-dependent shifts	± 0.5
Random measurement error (1 hr)	± 0.6
2nd harmonic distortion of servo modulation	± 0.5
Miscellaneous servo system effects	± 1.5
Multiplier chain transient phase shifts	± 1.0
Total 3σ estimate of uncertainty (square root of sum of squares)	± 3.2